Scientific Research Report

Single-Cell and Machine Learning Analysis Reveal Novel Inflammatory Macrophage Subtypes and Biomarkers in Periodontitis

Shaoyong Chen [a,b,†], *Jun Zhao* [c,†], *Jiayi Hang* [c,†], *Jianjia Tang* [d], *Rong Xiang* [d], *Siqin Zhang* [b,d*]

[a] *Department of Preventive Dentistry, College & Hospital of Stomatology, Guangxi Medical University, Nanning, Guangxi, China*
[b] *Guangxi Key Laboratory of Oral and Maxillofacial Rehabilitation and Reconstruction, Nanning, Guangxi, China*
[c] *Department of Oral and Maxillofacial Surgery, College & Hospital of Stomatology, Guangxi Medical University, Nanning, Guangxi, China*
[d] *Department of Oral Implantology, College & Hospital of Stomatology, Guangxi Medical University, Nanning, Guangxi, China*

ARTICLE INFO

Article history:
Received 9 July 2025
Received in revised form
30 August 2025
Accepted 1 October 2025
Available online xxx

Keywords:
Periodontitis
Macrophage heterogeneity
Single-cell RNA sequencing
Machine learning
Biomarkers
Inflammation

ABSTRACT

Background: Periodontitis (PD) is a chronic inflammatory disease marked by immune dysregulation and progressive tissue destruction. Macrophages play a pivotal role in PD pathogenesis; however, their heterogeneity, molecular characteristics and clinical relevance remain incompletely understood.

Objective: To identify and characterise novel subpopulations of macrophages associated with PD and explore their diagnostic and prognostic significance using single-cell RNA sequencing and machine learning.

Methods: Single-cell RNA sequencing (scRNA-seq) was performed on gingival tissues from PD patients and healthy controls to identify macrophage subtypes. Pseudotime trajectory and cell-cell communication analyses were conducted to investigate functional states and intercellular interactions. Metabolic pathway analysis assessed the metabolic features of PD-related macrophages (PD-MΦ). Machine learning algorithms were used to identify key diagnostic genes and construct a PD-MΦ-related gene signature (PMRGS). The model was validated using ROC analysis and in vitro experiments in THP-1-derived macrophages under inflammatory stimulation.

Results: Distinct PD-MΦ subpopulations were identified, exhibiting pro-inflammatory and immunometabolic alterations. Five diagnostic biomarkers – CXCR4, ATF3, TXN, CBX3 and MBP – were selected to develop the PMRGS. The gene signature showed strong diagnostic performance (area under the curve = 0.88). In vitro validation confirmed differential gene expression patterns consistent with scRNA-seq results.

Conclusion: This study reveals novel PD-associated macrophage subtypes and identifies a predictive gene signature with potential clinical utility in early diagnosis and disease monitoring. These findings provide new insights into PD immunopathogenesis and suggest therapeutic targets for macrophage-directed interventions.

* *Corresponding author*. Department of Oral Implantology, College of Stomatology, Hospital of Stomatology, Guangxi Medical University, No.10 Shuangyong Road, Nanning 530021, Guangxi, China.
E-mail address: siqinzhang@sr.gxmu.edu.cn (S. Zhang).
Shaoyong Chen: http://orcid.org/0000-0003-1994-7408
Siqin Zhang: http://orcid.org/0000-0002-6797-7866

† Shaoyong Chen, Jun Zhao, and Jiayi Hang are co-first authors.
https://doi.org/10.1016/j.identj.2025.103983

Introduction

Periodontitis (PD) is a prevalent chronic inflammatory condition that results in the progressive destruction of the supporting structures of the teeth. Clinically, it is characterised by gingival inflammation, periodontal pocket formation, alveolar bone loss, tooth displacement and eventual tooth loss.[1] As the sixth most common disease worldwide, PD affects approximately 20% to 50% of the global population. Far from being a simple localised infection, PD reflects a multifaceted pathological process driven by host-microbe interactions.[2-4] Mounting evidence suggests that the host immune response, rather than the microbial insult itself, plays a predominant role in tissue damage and disease progression.[5] Macrophages serve as frontline immune sentinels within periodontal tissues. Through their potent phagocytic activity, they eliminate pathogens and cellular debris. However, their excessive activation can lead to the release of pro-inflammatory mediators, resulting in collateral damage to periodontal tissues and exacerbation of disease.[6,7] Despite advances in clinical interventions, conventional treatments that focus primarily on microbial removal often fail to produce lasting improvements or prevent disease recurrence.

Immune imbalance is a hallmark of PD, where chronic inflammation disrupts the equilibrium between host defence mechanisms and tissue integrity. This dysregulation is driven by persistent immune cell activation, excessive cytokine secretion and sustained recruitment of inflammatory cells, culminating in the degradation of periodontal structures. Among these immune cells, macrophages are central to modulating both inflammation and tissue homeostasis. In addition to their role in pathogen clearance and apoptotic cell removal, macrophages influence tissue remodelling and repair through trophic and regulatory functions. Traditionally, macrophages are classified into 2 primary phenotypes based on their activation states: M1 (classically activated) and M2 (alternatively activated).[8] M1 macrophages predominantly play pro-inflammatory roles and facilitate the removal of tumour cells and pathogens, whereas anti-inflammatory M2 macrophages support the repair of tissues following damage.[9,10] Marked phenotypic heterogeneity is observed among macrophages in distinct tissue environments as they adapt to pathological and physiological conditions. Under PD and other chronic inflammatory conditions, maintaining an appropriate M1/M2 macrophage balance is crucial to preserve proper immune regulatory activity, and this dynamic balance can affect disease progression.[7] M1 macrophages secrete an array of pro-inflammatory cytokines, such as tumour necrosis factor-α (TNF-α), interleukin-6 (IL-6) and IL-8, enhancing immunity in large part through the stimulation of Th1 cell responses. M2 macrophages, in contrast, release epidermal growth factor (EGF), vascular endothelial growth factor (VEGF) and other growth factors, thereby shaping tissue repair, regeneration and angiogenesis.[6,11,12] However, this binary classification is now recognised as overly simplistic and insufficient to capture the full spectrum of macrophage heterogeneity observed in different tissues and disease contexts.

Given these limitations, a more refined characterisation of macrophage subsets in PD is urgently needed. Despite their critical role, limited studies have examined the phenotypic landscape of macrophages in periodontal tissues, especially in the context of comparing diseased versus healthy states. A comprehensive understanding of macrophage heterogeneity and function in PD is essential to uncovering disease mechanisms and identifying novel therapeutic strategies. Recent advances in single-cell RNA sequencing (scRNA-seq) have revolutionised the ability to dissect cellular diversity in complex tissues.[13] Unlike bulk RNA sequencing, scRNA-seq enables high-resolution profiling of individual cells, allowing for the identification of rare subpopulations and the characterisation of their distinct transcriptional and functional states. However, the application of scRNA-seq to explore immune dysregulation and macrophage heterogeneity in PD remains limited.

In this study, scRNA-seq was leveraged to explore the transcriptional heterogeneity of macrophages in the periodontal tissues of PD patients. The aim of this approach was to define a PD-specific macrophage subpopulation (PD-MΦ), elucidate its molecular and metabolic characteristics, and map the signalling interactions that characterise these cells within the inflammatory microenvironment. Furthermore, high-dimensional network analyses and machine learning techniques

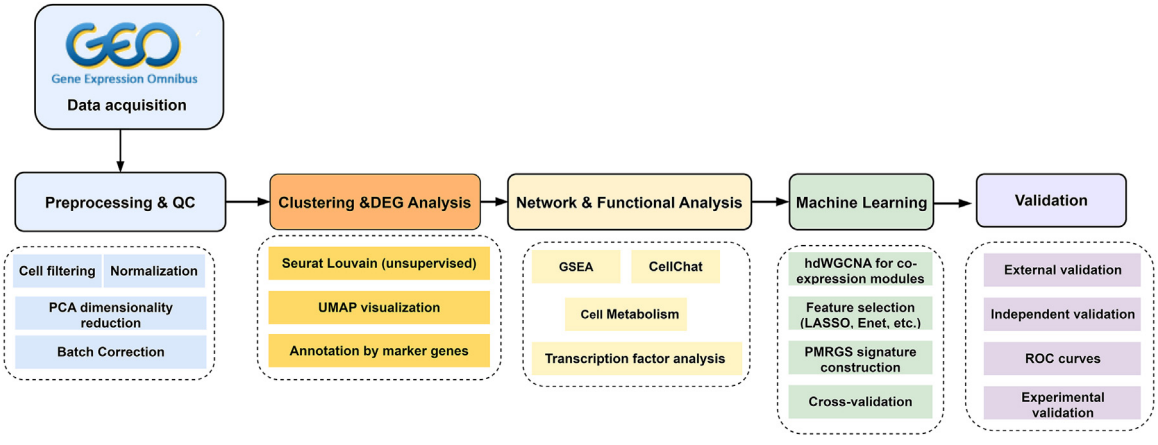

Fig. 1 – Workflow diagram of the analytical pipeline.

Sequential steps from scRNA-seq pre-processing and clustering to DEG identification, network analysis, machine learning –based feature selection, and validation in bulk datasets and in vitro experiments.

Table 1 – Analysed dataset overview.

Dataset	Year	Area	Species	Platform	Data type	Number of samples	
						Control	Periodontitis
GSE171213	2021	China	Homo	GPL24676	scRNA-seq	4	8
GSE10334	2008	USA	Homo	GPL570	Bulk microarray	64	183
GSE16134	2009	USA	Homo	GPL570	Bulk microarray	69	241
GSE106090	2017	China	Homo	GPL21827	Bulk microarray	6	12
GSE173078	2021	USA	Homo	GPL20301	Bulk RNA-seq	12	12

were employed to identify diagnostic gene signatures associated with these cells, and their expression was validated using both external datasets and in vitro inflammatory macrophage models. The overall analytical workflow of this study is presented in Figure 1. These findings offer new insights into the pathogenesis of PD and support the development of macrophage-targeted precision diagnostics and interventions.

Methods

Data acquisition and processing

Five publicly available gene expression datasets in total, including an additional RNA-seq cohort obtained from the NCBI Gene Expression Omnibus (GEO) database (http://www.ncbi.nlm.nih.gov/geo/) were used to conduct this study. The single-cell RNA sequencing dataset GSE171213 served as the primary resource for investigating macrophage heterogeneity in the periodontal tissues of both healthy individuals and PD patients.[14] Data pre-processing for scRNA-Seq data was carried out using the Seurat package in R, following established protocols.[15] Cells expressing fewer than 300 genes or more than 6500 genes in the dataset, as well as those with mitochondrial gene expression levels exceeding 10%, were excluded to ensure data quality while retaining the majority of informative cells. Gene expression normalisation and scaling were performed using the SCTransform function, followed by dimensionality reduction via principal component analysis (PCA).

To address batch effects arising from sample dissociation and processing, we applied the Harmony integration algorithm (v0.1.1) implemented in the Seurat package, using default parameters as previously described.[16] Harmony was selected for its robustness in integrating scRNA-seq datasets by effectively mitigating technical variation while preserving genuine biological heterogeneity. Unsupervised clustering and Uniform Manifold Approximation and Projection (UMAP) were subsequently employed to visualise and identify distinct cellular subpopulations. Cell-type annotations were assigned based on canonical marker genes or annotations from the original dataset publications. To evaluate the metabolic activity of identified cell populations, the scMetabolism package (version 0.2.1), which quantifies metabolic pathway activity at the single-cell level, was used. All data used in this study were de-identified and publicly accessible, and their use complies with NIH guidelines for exempt human subjects research under Category 4 (45 CFR 46.104).

The predictive model for this study was developed and validated using 3 bulk microarray datasets (GSE10334, GSE16134 and GSE106090, Affymetrix platforms). Normalised expression matrices provided by GEO (RMA pipeline with log2 transformation) were used for downstream analysis. In addition, an independent RNA-seq dataset (GSE173078, Illumina HiSeq 4000; 12 controls and 12 PD) was incorporated as an external validation cohort to assess cross-platform robustness of the PMRGS signature. For details regarding these datasets, see Table 1. As all data were publicly accessible, there was no requirement for patient consent or ethical approval.

Trajectory and intercellular interaction analyses

Unsupervised clustering and pseudotime trajectory inference were applied without predefined class labels, enabling a data-driven discovery of macrophage subtypes. To reconstruct the developmental trajectories of macrophage populations, the DDR-Tree algorithm from the Monocle R package (v2.26.0) was employed. Intercellular communication networks, particularly those involving macrophages associated with periodontitis, were inferred using the CellChat package (v1.6.1) with default parameters, following the standard workflow as recommended by the developers.[17]

Enrichment analyses

Differentially expressed genes (DEGs) among macrophage sub-clusters were identified using the FindMarkers function in the Seurat package. Subsequently, gene set enrichment analysis (GSEA) was performed using the clusterProfiler package. The enrichment results were visualised using the GseaVis package to elucidate the functional landscape of each subpopulation.

High-dimensional weighted gene co-expression network analysis (hdWGCNA)

To identify genes within the PD-associated macrophage (PD_macro) module that are also linked to psoriasis, a high-dimensional weighted gene co-expression network analysis was performed using the hdWGCNA package (v0.1.1.9010). The standardised analytical workflow detailed in the official tutorial was used to perform these analyses.[18] Metacells were constructed using the MetacellsByGroups function, aggregating 50 cells per metacell. For each macrophage-related cluster of interest, a subset of the Seurat object was used to execute the hdWGCNA pipeline, which included TestSoftPowers, ConstructNetwork, ModuleEigengenes, ModuleConnectivity and RunModuleUMAP, all run with default settings.

Table 2 – Primer sequences.

Gene	Forward (5′–3′)	Reverse (5′–3′)
CXB3	GGGATTTACAGAAAAGCTGGCA	TTGGTTTGTCAGCAGCATCTC
ATF3	TCACAAAAGCCGAGGTAGCC	ACTCTTTCTGCAGGCACTCC
CXCR4	TCCATTCCTTTGCCTCTTTTGC	AGGTGCAGCCTGTACTTGTC
TXN	ACTGTAACACCCAACCCAGC	GCACCGCTGACACCTCATAC
MBP	CCGGCAAGAACTGCTCACTA	CGACTATCTCTTCCTCCCAGC
β-actin	AGAAAATCTGGCACCACACCT	GATAGCACAGCCTGGATAGCA

PPI network and receiver operating characteristic curves

The STRING database (v10.5, http://string-db.org/) was utilised to construct the PPI network, which was visualised using Cytoscape (v3.8.0). Receiver operating characteristic (ROC) curves were plotted using the timeROC and survival packages (v1.3.1 and v2.1.2, respectively) to assess model performance.

Immune infiltration assessment

Immune landscape profiling was carried out using the GSVA package. To visualise intercellular correlations among 28 immune cell types, a correlation heatmap was generated using the corrplot package (v0.92). The relative abundance of each immune cell population was illustrated using ggplot2 (v3.4.1) and pheatmap (v1.0.12).

Machine learning model construction

Macrophages were clustered using Seurat's Louvain algorithm in an unsupervised manner, ensuring that transcriptional heterogeneity rather than prior assumptions guided sub-cluster delineation. Pseudotime trajectory analysis with Monocle was similarly performed without predefined labels. A consensus predictive model was devised by integrating 10 machine learning algorithms: elastic net (Enet), stepwise Cox regression, random survival forest (RSF), CoxBoost, lasso regression, ridge regression, partial least squares for Cox (plsRcox), supervised principal components (SuperPC), generalised boosted regression modelling (GBM) and survival support vector machine (survival-SVM). Model training was conducted using a leave-one-out cross-validation (LOOCV) approach across 101 algorithmic combinations. The GSE10334 dataset was used for training, while GSE16134 served as the validation cohort. To further strengthen robustness and minimise the potential impact of dataset overlap, we additionally validated the PMRGS signature in the GSE106090 microarray dataset, which yielded consistent diagnostic accuracy. Moreover, an independent RNA-seq dataset (GSE173078) was incorporated as an external validation cohort. The PMRGS maintained good diagnostic performance in this dataset (area under the curve [AUC] = 0.764), confirming its cross-platform generalisability (Supplementary Figure S2).

Cell culture and treatment

THP-1 monocytes were cultured in RPMI-1640 medium supplemented with 10% foetal bovine serum and 1% penicillin-streptomycin. Cells were maintained at 37 °C in a humidified atmosphere containing 5% CO_2. To induce macrophage differentiation, cells were seeded at a density of 1×10^6 cells/mL and treated with 100 ng/mL PMA for 24 hours. To simulate the inflammatory milieu of periodontitis, differentiated macrophages were exposed to 1 μg/mL lipopolysaccharide for 24 hours (PD group), while untreated cells served as the control.

qRT-PCR

Total RNA was isolated using TRIzol reagent, followed by cDNA synthesis using a reverse transcription kit. Quantitative reverse transcription PCR (qRT-PCR) was performed with SYBR Green PCR Master Mix. Expression levels of ATF3, CXCR4, TXN, CBX3 and MBP were normalised to β-actin. Relative gene expression was quantified using the $2^{-\Delta\Delta Ct}$ method. Primer sequences are listed in Table 2.

Western blotting

Proteins were extracted using RIPA buffer containing protease inhibitors. Equal amounts of protein (30 μg/sample) were resolved by SDS-PAGE, transferred onto PVDF membranes and incubated overnight with primary antibodies specific for ATF3 (CST, #18665, 1:1500), CXCR4 (Abcam, ab181020, 1:1000), TXN (CST, #14907, 1:800), CBX3 (Abcam, ab217999, 1:1500), MBP (Abcam, ab11159, 1:800) and β-actin. Membranes were then incubated with HRP-conjugated secondary antibodies, and immunoreactive bands were visualised using an enhanced chemiluminescence detection system. Band intensity was quantified using ImageJ software.

Statistical analyses

All statistical procedures and visualisations were performed using R software (v4.2.1). Pearson correlation analysis was used to assess relationships between continuous variables. For comparisons between groups, 2-tailed Student's t-tests or one-way ANOVA followed by Tukey's post hoc test were used as appropriate. A P-value $< .05$ was deemed significant.

Results

Single-cell transcriptomic profiling reveals cellular composition alterations in periodontitis

To characterise the cellular heterogeneity of periodontal tissues from both healthy individuals and patients with PD, scRNA-seq data obtained from affected tissues were analysed. After rigorous quality control and batch correction, a total of 33,405 high-quality cells expressing 21,472 genes were

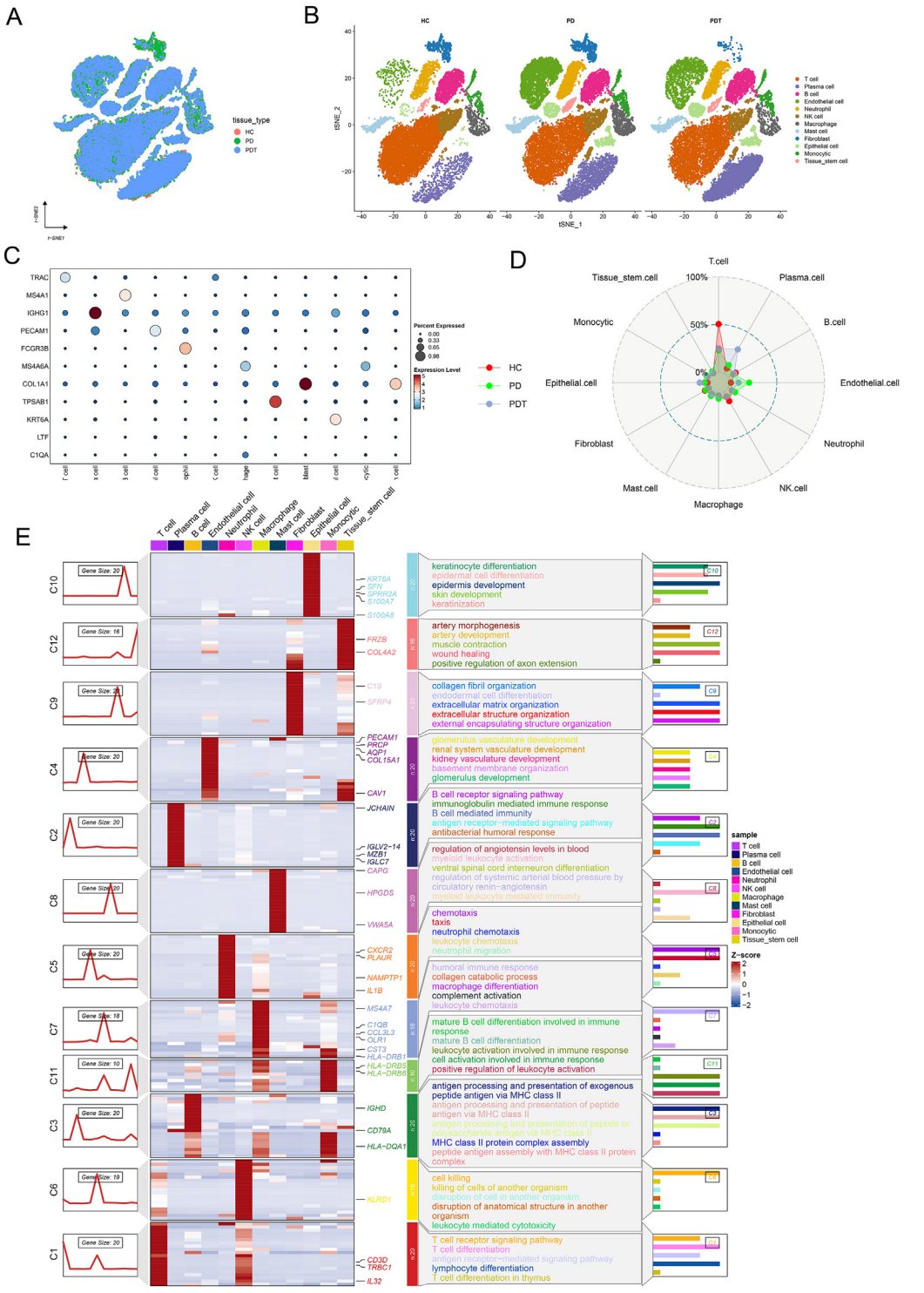

Fig. 2 – Alterations of the cellular composition from human periodontal tissues of HCs, PDs and PDTs, according to dataset GSE171213. A, t-SNE visualisation showing cell clusters organised from HCs, PDs and PDTs periodontal tissue. B, Unbiased clustering separates cells into 16 distinct populations, each marked by a unique colour. C, Dot plot illustrating differentially expressed genes (DEGs) changes in each cell population. D, Proportion of different cellular clusters among the HCs, PDs and PDTs periodontal tissue. E, Left panel: Dynamic patterns of representative DEGs for each cell population. Middle panel: Heatmap showing the representative DEGs across each cell population. Right panel: Representative enriched gene ontology (GO) terms for each cell population.

retained for analysis. As shown in supplementary figure S1, PCA and UMAP visualisations confirmed that batch-associated clustering was effectively minimised after Harmony integration, while biologically meaningful cell-type–specific patterns were preserved. These cells were classified into 12 distinct clusters based on canonical marker gene expression,

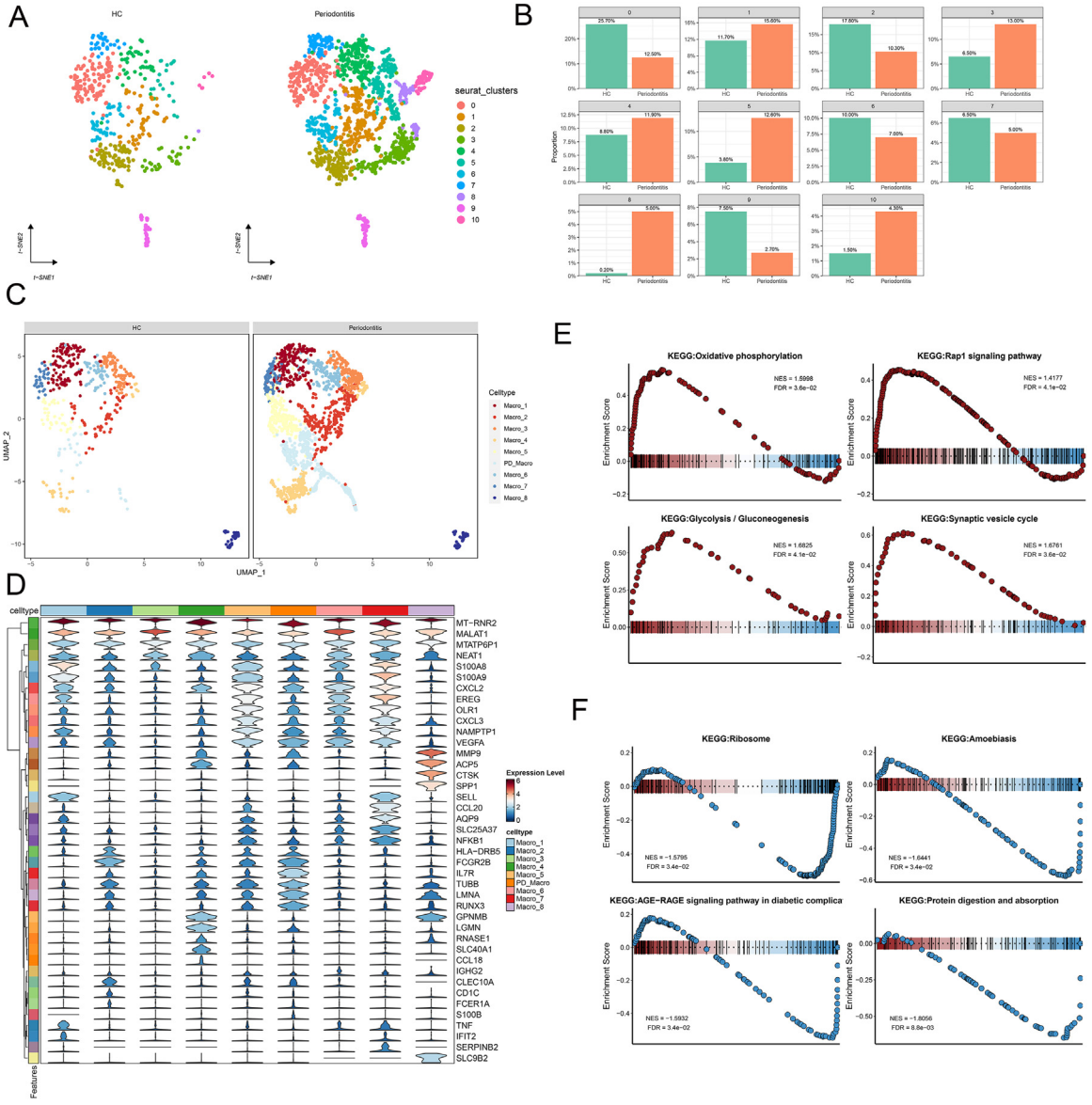

Fig. 3 – Single-cell analysis reveals the heterogeneity of macrophages in PD periodontal tissues. A, t-SNE plot showing the distribution of 11 macrophages sub-clusters in HC and PD periodontal tissues. B, Proportions of macrophage sub-clusters in PD compared to HC tissues. C, UMAP diagram displaying the distribution of further identified 9 macrophage sub-clusters in HC and PD periodontal tissues. D, Heatmap for the gene changes in each macrophage sub-cluster. E and F, GSEA enrichment plots of representative signalling pathways upregulated (E) and downregulated (F) in PD-related macrophages compared to HC macrophages.

corresponding to T cells, B cells, plasma cells, monocytes, NK cells, mast cells, endothelial cells, fibroblasts, epithelial cells, macrophages, neutrophils and tissue stem cells (Figure 2A-C). The changes in cellular composition across healthy control (HC), PD and post-treatment (PDT) tissue samples were then assessed (Figure 2D). Notably, PD tissues exhibited a marked increase in endothelial cells, NK cells, macrophages, plasma cells, epithelial cells, monocytes and mast cells. In contrast, the abundance of T cells, B cells and tissue stem cells was significantly reduced.

To further characterise the transcriptional profiles of each cell type, gene activity scores were computed based on relative expression, and unsupervised clustering analyses were performed. This analysis yielded 12 distinct gene expression patterns, each enriched for specific biological functions (Figure 2E). Among these, cluster 7 exhibited a strong macrophage-specific expression signature, enriched for pathways involved in humoral immunity, collagen degradation, macrophage differentiation, complement activation and leukocyte chemotaxis.

Characterisation of macrophage sub-cluster heterogeneity in periodontitis

To gain deeper insights into macrophage-specific responses in PD, macrophages were isolated and t-SNE clustering was

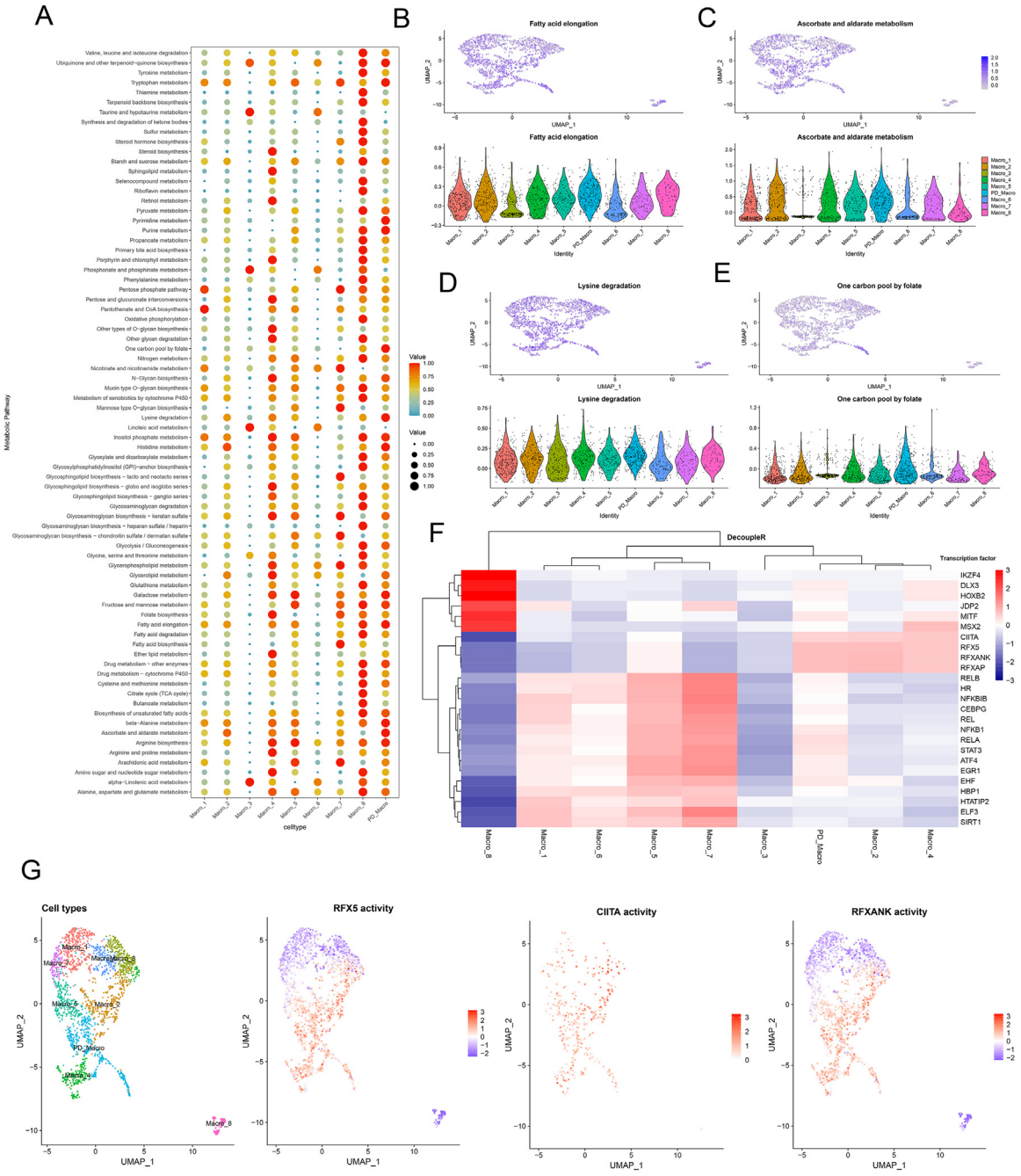

Fig. 4 – A, Dot plot depicting the activation status of metabolic pathways for each macrophage subtype. B-E, Top 4 significantly enriched metabolic pathways in PD-associated macrophages, including in fatty acid elongation (B), ascorbate and aldarate metabolism (C), lysine degradation (D) and one carbon pool by folate (E). F, Heatmap of transcription factor analysis scores in the 9 macrophage subtypes. G, UMAP plot displaying the distinct activation patterns of transcription factors (RFX5, CIITA and RFXANK) in PD-related macrophage sub-clusters.

conducted, revealing 11 distinct subpopulations (Figure 3A, B). Among these, sub-clusters 5, 8 and 10 were significantly enriched in PD samples compared to HC tissues and were therefore classified as PD-associated macrophages (PD-MΦ) (Figure 3B, C). A heatmap illustrating the differential expression of key genes across macrophage subsets is shown in Figure 3D, highlighting elevated levels of MT-RNR2 and MALAT1 in PD-MΦ clusters.

Gene set enrichment analysis (GSEA) of highly expressed genes in PD-MΦ was next conducted in an effort to explore the underlying mechanisms through which these cells function. This approach revealed that these genes exhibited significant enrichment in pathways related to oxidative phosphorylation, Rap1 signalling, glycolysis/gluconeogenesis and synaptic vesicle cycling (Figure 3E). Conversely, pathways such as protein digestion and absorption, ribosome function, amoebiasis and

the AGE-RAGE signalling axis were downregulated (Figure 3F). Metabolic pathway analysis revealed notable enrichment in fatty acid elongation, lysine degradation, ascorbate and aldarate metabolism and folate-mediated one-carbon metabolism within PD-MΦ populations (Figure 4A-E). Moreover, transcription factor analysis demonstrated the activation of distinct regulatory factors: RFX5 in PD_Macro, CIITA in Macro_2 and RFXANK in Macro_4 (Figure 4F, G), suggesting transcriptional reprogramming as a key feature of macrophage heterogeneity in periodontitis.

Pseudo-time trajectory and CellChat analyses

To investigate the developmental origins and progression of PD-MΦ, a pseudotime trajectory analysis was conducted. This analysis revealed the distinct positioning of PD-MΦ at the terminal end of the differentiation continuum (Figure 5A-C), while macrophage clusters 4, 5 and 7 were predominantly located at early stages. These results suggest that PD-MΦ follows a unique developmental trajectory compared to other macrophage subsets. Further clustering of differentially expressed genes (DEGs) based on their temporal expression patterns along the pseudotime axis uncovered 4 distinct gene expression profiles (Figure 5D). To elucidate the communication dynamics between PD-MΦ and other cell types, CellChat, a computational framework for inferring intercellular signalling, was next employed. This analysis demonstrated that PD-MΦ were highly interactive, engaging in widespread communication with a variety of immune and stromal populations (Figure 4E). Specifically, PD-MΦ were found to engage in direct signalling through multiple ligand-receptor pairs, including GRN-SORT1 and MIF−(CD74 + CD44) (Figure 5F, G). Additionally, the signalling pathways mediated by GypA, GALECTIN and ANNEXIN were markedly upregulated in interactions involving PD-MΦ, indicating their central role in coordinating cellular responses within the periodontal microenvironment (Figure 5H-J).

hdWGCNA-based identification of PD-MΦ-related hub gene modules

To gain further insight into the functional roles of PD-MΦ, hdWGCNA was conducted. By applying a soft-threshold power of 20, a scale-free network topology was established (Figure 6A) and 15 gene co-expression modules were identified (Figure 6B, C). Of these, 5 modules (brown, turquoise, salmon, green and black) exhibited a strong correlation with the PD-MΦ population, suggesting functional relevance to this specific macrophage subset (Figure 6D). To better understand the inter-module relationships, the pairwise correlations were visualised using both a correlation heatmap and a PPI network (Figure 6E, F).

Machine learning-based screening for PD-MΦ signature genes

To pinpoint critical genes associated with PD-MΦ, LASSO regression was implemented based on the hub genes previously identified via hdWGCNA. Analysis of an external bulk RNA-seq dataset (GSE10334) yielded 22 candidate genes with potential prognostic value in periodontitis. These genes were subsequently mapped to their respective chromosomal locations, which were found to be distributed across 13 chromosomes (Figure 7B). Construction of a PPI network from these candidates highlighted 5 core genes associated with the prognostic outcomes of patients with PD, including TXN, ATF3, CXCR4, CBX3 and MBP, suggesting their involvement in disease pathology (Figure 7C, D). Their expression levels were further assessed using violin plots, revealing significantly elevated expression of ATF3 and CXCR4 in PD patients, while TXN, CBX3 and MBP were significantly downregulated (Figure 7E).

Analysis of immune cell infiltration in periodontitis

To characterise the immune landscape of PD-affected tissues, immune infiltration analysis was performed using the GSEA algorithm. Comparative assessment of proportional immune cell frequencies between PD and healthy tissues revealed increased infiltration of several immune subsets in the PD group, including myeloid-derived suppressor cells (MDSCs), activated CD8+ and CD4+ T cells, central memory CD8+ T cells, Th1 cells, activated and immature B cells (Figure 8A-E). In contrast, there was a marked reduction in monocytes, immature dendritic cells, $CD56^{bright}$ and $CD56^{dim}$ NK cells, $\gamma\delta$ T cells, T follicular helper cells, effector memory CD4+ T cells, Th2 and Th17 cells, mast cells, neutrophils and memory B cells. A correlation heatmap further illustrated the relationship between the 5 core PD-MΦ genes and immune cell types (Figure 8F). Interestingly, these genes displayed diverse correlation patterns. For instance, CXCR4 was positively associated with the majority of immune cells, while TXN, CBX3 and MBP showed predominantly negative correlations. These opposing trends suggest distinct regulatory roles for these genes in immune modulation within the context of PD.

Prognostic value of the PD-MΦ gene signature in periodontitis

To evaluate the prognostic potential of PD-MΦ-associated genes, a composite PD-MΦ-related gene score (PMRG score) was calculated in both healthy and PD-affected periodontal samples. The PMRG score was significantly higher in the PD group, implicating this gene set in disease development (Figure 9A). ROC curve analysis demonstrated that each of the 5 signature genes – CBX3, CXCR4, TXN, MBP and ATF3 – as well as the combined PMRG score, yielded AUC values exceeding 0.65, indicating strong diagnostic utility (Figure 9B-F, I). To identify the most robust predictive model, a Leave-One-Out Cross-Validation (LOOCV) framework was utilised to evaluate 101 machine learning algorithm combinations. The GSE10334 dataset was used for model training, while GSE16134 served as the validation set. Each model's performance was assessed using the concordance index (C-index), and the Stepwise Cox regression combined with Gradient Boosting Machine (StepCox + GBM) emerged as the optimal model, achieving an average C-index of 0.88 ($P < .0001$; Figure 9G-I). To further strengthen robustness and reduce the potential impact of dataset overlap, we additionally validated the PMRGS signature in the GSE106090 microarray dataset, which yielded consistent diagnostic accuracy. Moreover, an

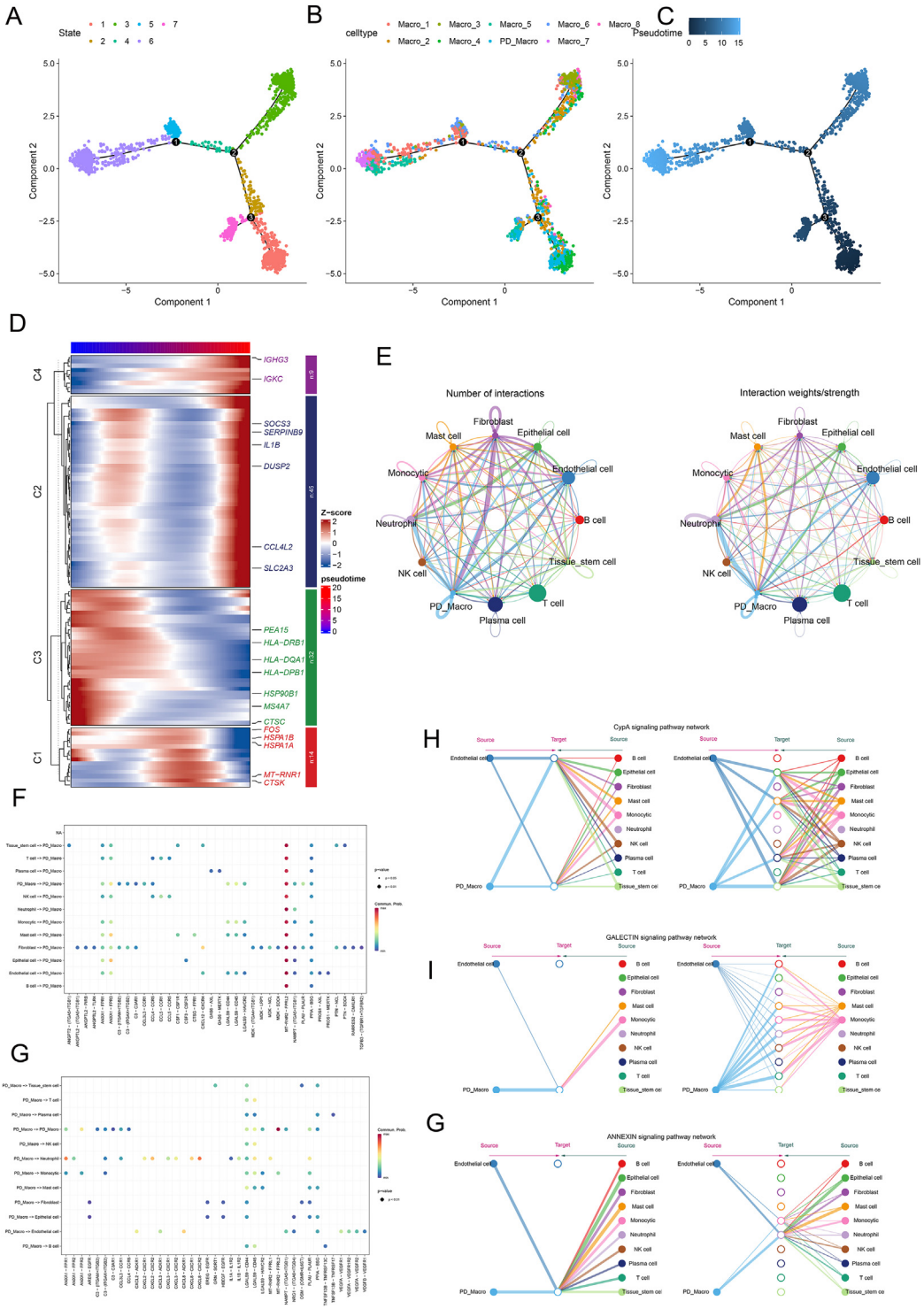

Fig. 5 – Trajectory and intercellular communication analysis of macrophages and other subtypes in PD patients. A-D, The analysis of macrophages developmental trajectory, color-coded by states (A), cellular subtypes (B), and pseudotime (C). D, Heatmap depicting clusters of dynamic gene expression patterns over pseudotime. E-J, Intercellular communication analysis in AT2 cell subpopulations. E, Circle plots illustrating the number (left) and strength (right) of interactions across all cell subtypes. F and G, Dot plot showing predicted ligand–receptor interactions between PD-related macrophages and other cell populations. H-J, Hierarchical plots exhibiting the inferred cell-cell communication networks for CypA (H), GALECTIN (I) and ANNEXIN signalling pathways (J).

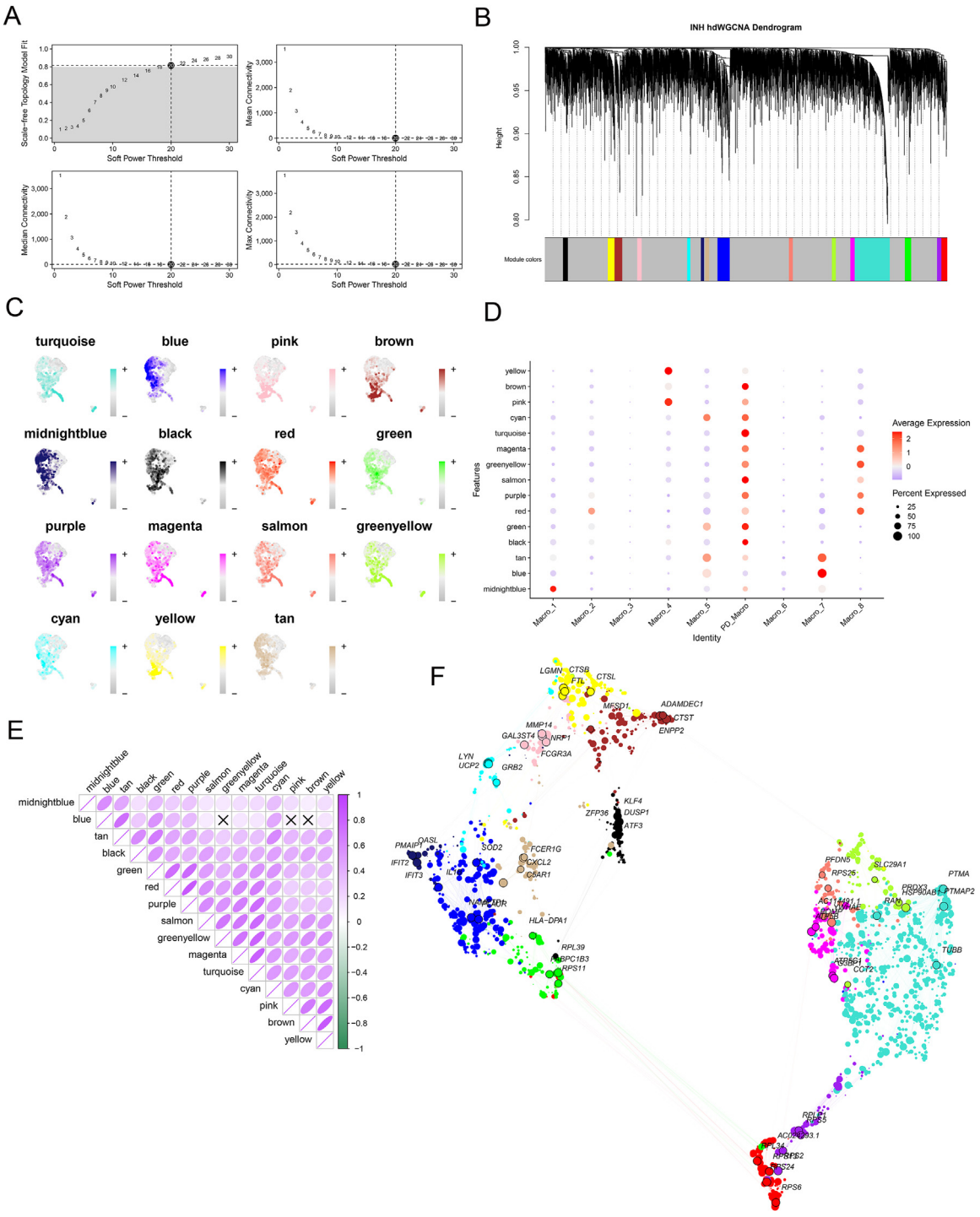

Fig. 6 – Identification of the hub modules for PD-MΦ through the hdWGCNA.

A, Establishment of a scale-free network with an optimal soft-threshold power of 20. B, Classification of highly variable genes into 15 modules by the hdWGCNA. C, t-SNE plots depicting distribution of crucial genes expression of per module. D, Assessment of module activity across different macrophage subtypes through hdWGCNA. E, The matrix plot intuitively visualising the correlation of inter-module relationships. F, A UMAP plot depicting the co-expression network among twelve gene modules. The top 4 hub genes of each module are annotated.

independent RNA-seq dataset (GSE173078) was incorporated as an external validation cohort. The PMRGS maintained good diagnostic performance in this dataset (AUC = 0.764), confirming its cross-platform generalisability (Supplementary Figure S2).

Validation of key genes in periodontitis-associated macrophages

To experimentally validate the expression of key PD-MΦ-associated genes, qRT-PCR and Western blotting analyses

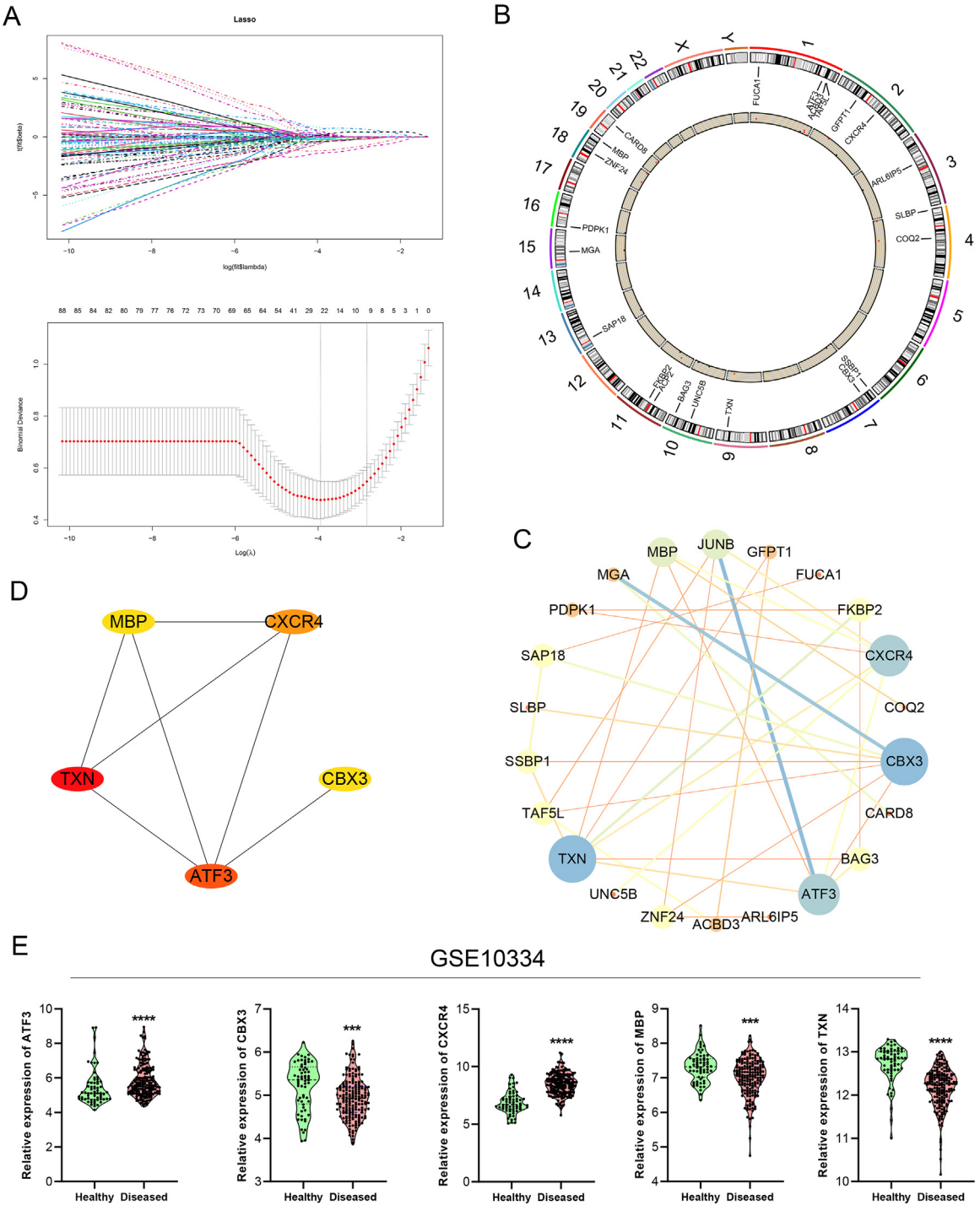

Fig. 7 – Identification of hub genes associated with PD-MΦ. A, Twenty-two candidate key genes identified using LASSO regression. B, Chromosomal locations of the 22 candidate key genes. C, PPI network construction of the 22 candidate key genes. D, PPI network highlighting the top 5 candidate hub genes. E, Violin plot displaying the gene expression levels of the top 5 candidate genes.

were performed using THP-1-derived macrophages exposed to normal or periodontitis-mimicking inflammatory conditions. Western blotting revealed increased protein levels of ATF3 and CXCR4, while TXN, CBX3 and MBP were significantly reduced under inflammatory conditions (Figure 10A-G). These results were consistent with qRT-PCR findings, which showed transcriptional upregulation of ATF3 and CXCR4, along with downregulation of TXN, CBX3 and MBP in macrophages subjected to periodontitis-like stimuli (Figure 10H-L). Collectively, these findings support the involvement of these genes in key processes such as immune modulation, oxidative stress response and

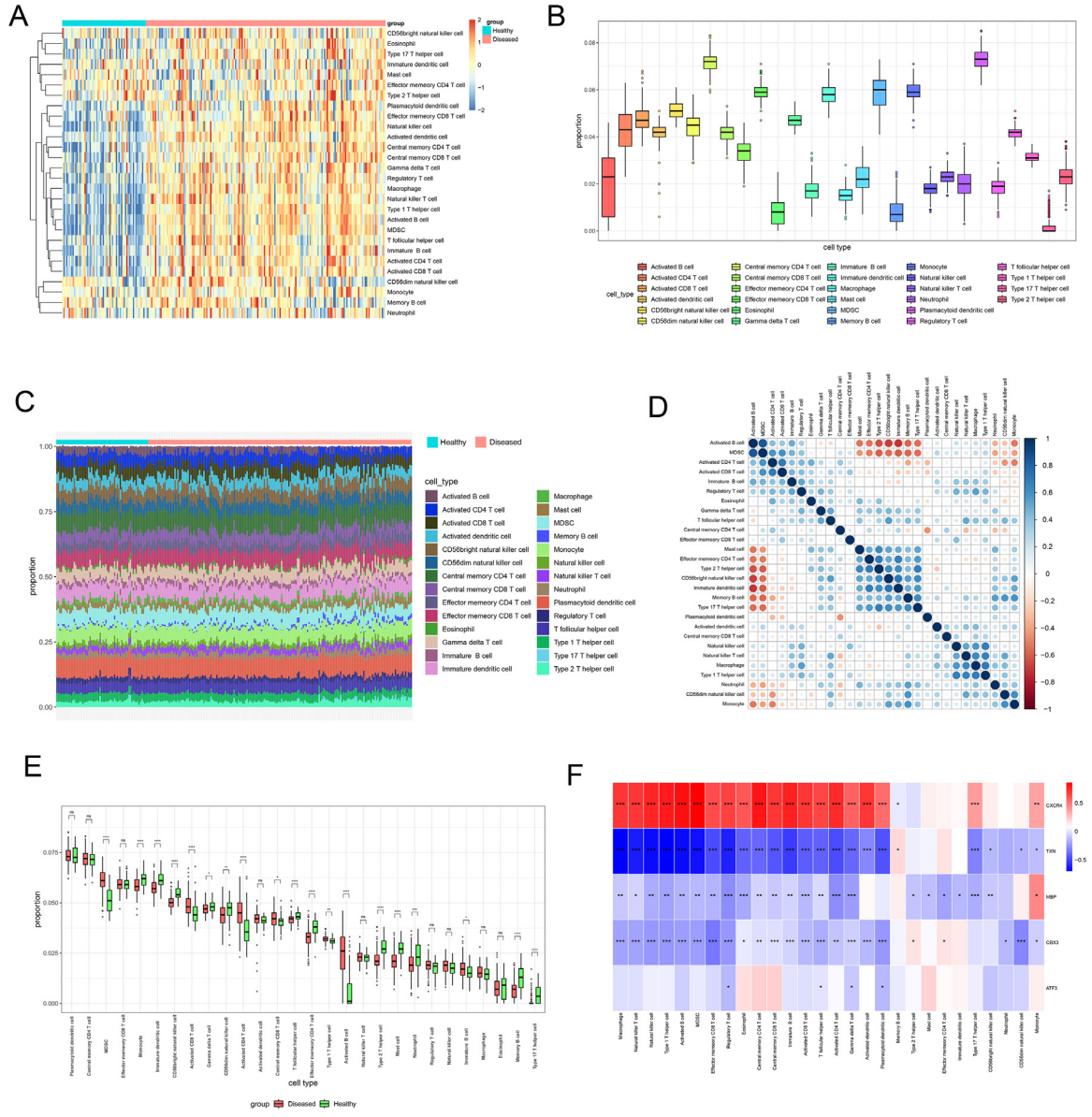

Fig. 8 – Immune cell infiltration analysis. A, Heatmap, (C) stacked bar chart and (E) bar plot comparing immune cell infiltration between the diseased and healthy groups in periodontal tissues. B, Relative proportions of 28 immune cell types. D, Correlation matrix among the 28 immune cell types. F, Correlation heatmap showing the relationship between 5 hub genes and immune cell infiltration. Blue represents a negative correlation, and red represents a positive correlation. *P < .05, **P < .01, ***P < .001.

chromatin dynamics in PD-associated macrophages, providing critical evidence for their contribution to disease progression.

Discussion

In this study, a previously uncharacterised subset of macrophages associated with periodontitis (PD-MΦ) was identified and distinguished by unique metabolic adaptations and immunomodulatory functions that appear to promote chronic inflammatory responses in periodontal disease. This analysis revealed a notable enrichment of PD-MΦ within diseased periodontal tissues. Their transcriptional profile indicates a pivotal role in sustaining the local inflammatory milieu, modulating immune dynamics and contributing to tissue degradation. A major finding of this investigation was the altered composition of immune cells in PD lesions. Specifically, a pronounced accumulation of macrophages and NK cells was observed, indicative of heightened innate immune activity. This activation likely stems from persistent microbial stimuli and is further propagated by pro-inflammatory mediators such as TNF-α and IL-1β, which together create a self-perpetuating cycle of inflammation.[11,19] Conversely, the observed decline in T and B lymphocyte populations suggests dysfunction within adaptive immunity, potentially due to

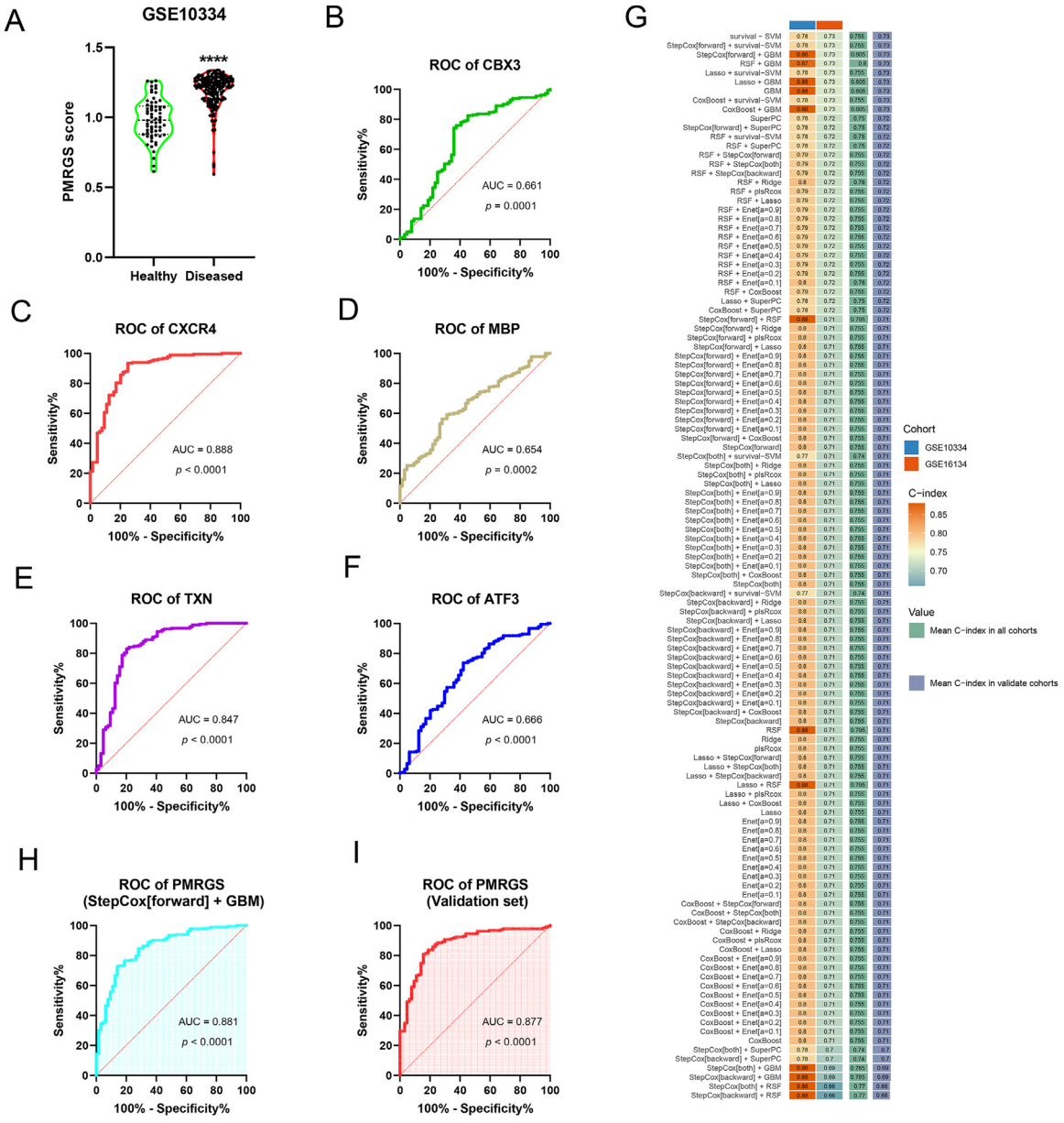

Fig. 9 – Construction and validation of a PMRGs diagnostic model. A, Violin plot depicting the PMRGs score levels in periodontal tissues of patients with PD (*n* = 183) and healthy controls (*n* = 64). Data are presented as means ± SD, **** P < .0001 vs control. B-F, ROC curves for (B) CBX4, (C) CXCR4, (D) MBP, (E) TXN and (F) ATF3 for external dataset validation. G, Identification of the optimal model using the average AUC from 101 diagnostic models across all training and test datasets. H-I, Leave-one-out cross-validation (LOOCV) framework was used to generate 101 prediction models, and the C-index was calculated for each model on both training and validation datasets. J, ROC curve for the PMRGs associated with PD-MΦ.

exhaustion or a phenotypic shift favouring pro-inflammatory Th17 cells – a phenomenon previously linked to tissue damage in chronic inflammatory states.[20] Furthermore, the reduction in stem cell populations within periodontal tissues implies impaired regenerative capacity, consistent with prior studies highlighting inflammation-induced suppression of tissue repair mechanisms.[21,22]

A key methodological strength of this study is the use of label-free machine learning approaches, including unsupervised clustering and pseudotime trajectory inference, which minimised subjective annotation bias and enabled the unbiased discovery of PD-MΦ. Unlike traditional M1/M2 paradigms or supervised frameworks requiring predefined labels, our data-driven strategy prioritised intrinsic transcriptional patterns of 33,405 single cells. This allowed macrophages to be resolved into 11 distinct sub-clusters, with PD-MΦ (clusters 5, 8 and 10) only identified post hoc by their enrichment in PD samples and unique molecular signatures. Pseudotime analysis further positioned PD-MΦ at a distinct terminal trajectory, insights that would not have been achievable using hypothesis-driven or label-dependent methods. Detailed characterisation of macrophage subpopulations revealed substantial

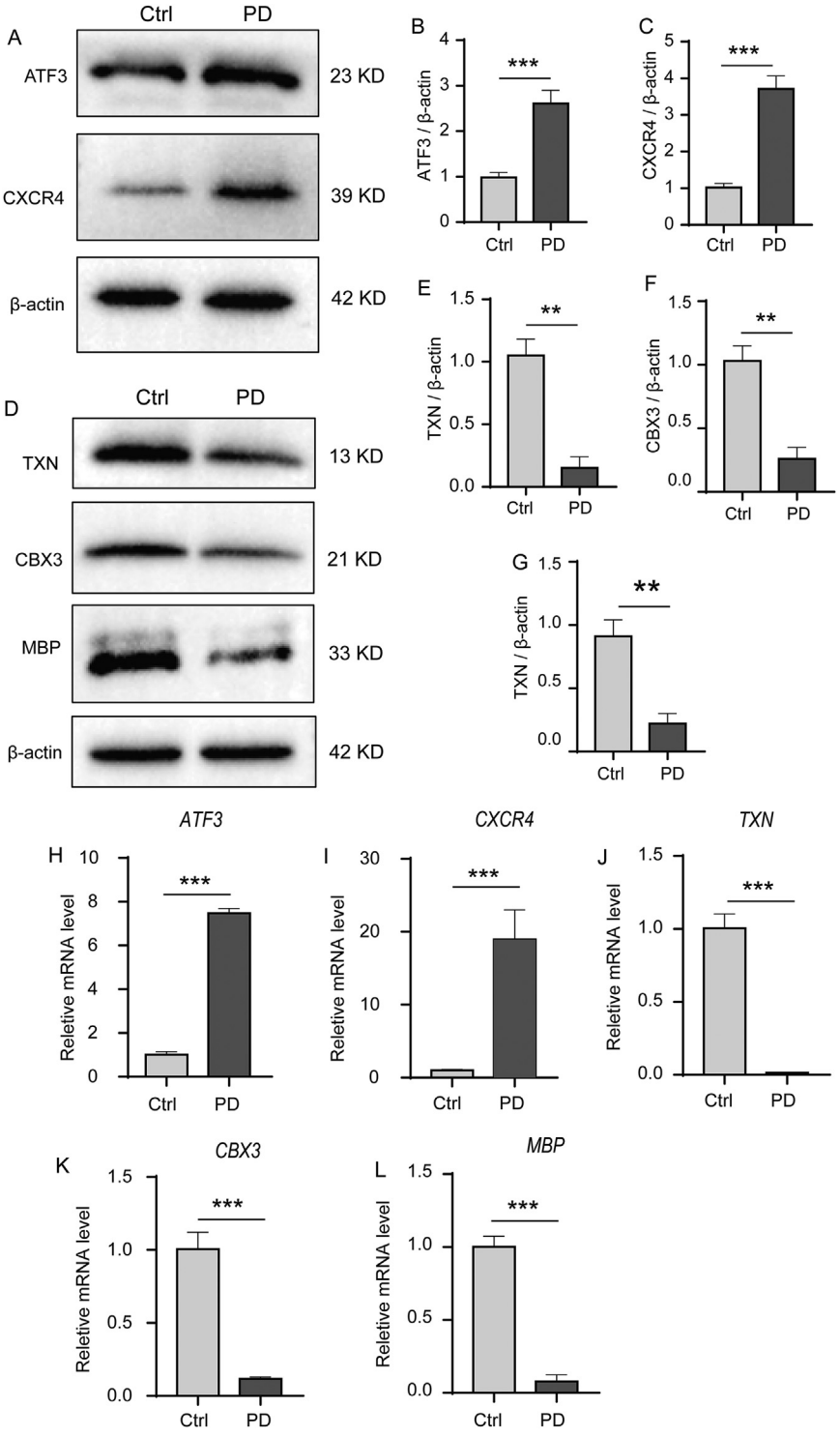

Fig. 10 – Expression levels of hub genes in periodontitis macrophages. A-G, The protein expression of ATF3, CXCR4, TXN, CBX3 and MBP. E-K, The mRNA expression of ATF3, CXCR4, TXN, CBX3 and MBP. Values represent the mean ± SD; $^{**}P < .01$, $^{***}P < .001$.

heterogeneity, leading to the identification of the novel PD-MΦ subset. Transcriptomic profiling of these cells showed elevated expression of MT-RNR2 and MALAT1, both of which have recognised roles in immune regulation. MT-RNR2 encodes humanin, a mitochondrial-derived peptide known for its anti-inflammatory effects and regulatory influence on mitochondrial function.[23,24] Its upregulation may represent an adaptive mechanism to counterbalance mitochondrial stress, highlighting mitochondrial stability as a potential target in PD therapy. Meanwhile, MALAT1, a long non-coding RNA implicated in immune cell polarisation and cytokine regulation,[25,26] was also significantly elevated. This

increase may amplify inflammatory signalling and contribute to the progressive destruction of periodontal tissue. Together, these findings emphasise the immunoregulatory roles of MT-RNR2 and MALAT1 in the pathophysiology of PD.

GSEA further demonstrated that PD-MΦ undergo pronounced metabolic reprogramming. Specifically, these cells exhibited enhanced activity in oxidative phosphorylation, Rap1 signalling and glycolysis/gluconeogenesis, while pathways related to protein digestion, absorption and AGE-RAGE signalling were suppressed. These shifts likely reflect an adaptation to the high-energy demands of chronic inflammation. Oxidative phosphorylation fuels ATP production necessary for sustaining pro-inflammatory signalling, whereas glycolysis accelerates the synthesis of inflammatory mediators, exacerbating tissue damage. Rap1, a small GTPase involved in integrin signalling and cellular adhesion, may enhance immune cell recruitment to inflamed periodontal sites, thereby amplifying local immune responses.[27,28] Interestingly, suppression of the AGE-RAGE pathway, typically implicated in diabetic inflammation, suggests a distinct metabolic reconfiguration in the PD microenvironment.

Additional metabolic alterations in PD-MΦ included upregulation of fatty acid elongation, lysine degradation, ascorbate and aldarate metabolism and the folate-driven one-carbon pool pathway. These changes further reflect the metabolic flexibility of PD-MΦ in adapting to inflammatory conditions. Fatty acid elongation supports the generation of lipid mediators essential for macrophage activation and polarisation.[29,30] The observed increase in lysine degradation, a pathway linked to immune signalling and epigenetic modulation,[31] may indicate reprogramming at the transcriptional level in response to sustained inflammatory cues. Enhanced ascorbate metabolism suggests an adaptive response to oxidative stress,[32] while upregulation of the folate pathway supports nucleotide biosynthesis and methylation processes, enabling macrophage proliferation and inflammatory gene expression.[33,34] Collectively, these metabolic rewiring events establish a feedback loop that reinforces the inflammatory phenotype of PD-MΦ and promotes progressive tissue destruction.

Beyond metabolic changes, transcriptional regulatory analysis revealed elevated activity of key transcription factors including RFX5, CIITA and RFXANK, which are central regulators of MHC class II gene expression and antigen presentation. Their upregulation implies a heightened antigen-presenting capacity in PD-MΦ, potentially enhancing CD4+ T cell activation and prolonging inflammation. Overexpression of MHC class II-related genes may also enable immune evasion by oral pathogens, contributing to their persistence within periodontal niches.[35-37] Moreover, components of the RFX complex, including RFX5 and RFXANK, have been shown to downregulate extracellular matrix (ECM)-related genes such as COL1A2 in response to IFN-γ, possibly impairing tissue integrity during chronic inflammation.[38] These findings underscore the dual roles of PD-MΦ in bridging innate and adaptive immune responses while simultaneously influencing ECM remodelling and tissue degradation. Cell-cell communication analysis further illuminated the central role of PD-MΦ in orchestrating inflammatory signalling networks. Key ligand-receptor interactions, including GRN−SORT1 and MIF−(CD74/CD44), were prominent. GRN (progranulin), a precursor growth factor, signals through SORT1 to regulate macrophage proliferation and activation,[39] potentially fuelling chronic inflammation. Meanwhile, MIF signalling via CD74 and CD44 is known to promote macrophage survival, chemotaxis and cytokine production through pathways such as ERK1/2 and PI3K/AKT.[40,41] These interactions likely amplify immune cell recruitment and activation, further entrenching the inflammatory state and exacerbating tissue destruction. Altogether, these data position PD-MΦ as central regulators of the immunopathology of periodontitis, offering a high-resolution cellular map that enhances the current understanding of disease mechanisms and reveals promising targets for therapeutic intervention. Building on these insights, hdWGCNA and machine learning approaches were applied to identify a gene signature uniquely associated with PD-MΦ. Five key genes (ATF3, CXCR4, TXN, CBX3 and MBP) emerged as potential biomarkers of disease progression. The PD-MΦ-related gene (PMRG) score, derived from these markers, was positively correlated with disease severity, underscoring its prognostic utility. Among the identified genes, CXCR4 and ATF3 were markedly upregulated in PD tissues. Prior studies have shown that CXCR4 plays a critical role in immune cell trafficking, promoting macrophage and T cell infiltration into inflamed periodontal pockets, thereby exacerbating tissue destruction.[42,43] ATF3, a transcription factor induced by cellular stress, is implicated in modulating inflammatory responses and has been found to be elevated in PD models, suggesting a role in inflammation-driven tissue damage.[44] In vitro assays using THP-1-derived macrophages confirmed increased expression of CXCR4 and ATF3, along with reduced levels of TXN, CBX3 and MBP under periodontitis-like conditions. These results provide functional support for their involvement in PD-MΦ phenotype and disease pathogenesis. However, further mechanistic studies are warranted to delineate their precise roles in PD progression.

This study also has several limitations that should be acknowledged. First, 2 of the validation datasets (GSE10334 and GSE16134) were derived from the same periodontal tissue archive and may contain multiple samples from individual patients. Because patient-level identifiers are not available in the public repositories, we cannot completely exclude the possibility of sample overlap or non-independence. Importantly, our key conclusions are not solely dependent on these 2 datasets, as consistent results were obtained when each dataset was analysed separately and further confirmed in additional cohorts. To minimise this risk, we applied dataset-specific training/validation strategies and incorporated GSE106090 as well as an independent RNA-seq dataset (GSE173078) for external validation, which consistently supported the diagnostic value of the PMRGS signature. Second, the bulk microarray datasets inherently differ from RNA-seq in signal generation and dynamic range; although we applied standard normalisation procedures and demonstrated cross-platform robustness, these technical differences may still influence gene expression quantification. Finally, while our scRNA-seq and in vitro experiments

provide strong support for the identified PD-MΦ subsets and biomarkers, future large-scale cohorts with complete clinical metadata, as well as spatial transcriptomic and in vivo functional validation, will be critical to fully substantiate and generalise these findings.

Conclusion

In conclusion, this study identifies a novel subset of macrophages, PD-MΦ with distinct metabolic and immunological characteristics that contribute to the development and persistence of periodontitis. Leveraging single-cell RNA sequencing and integrative machine learning techniques, a PD-MΦ-specific gene signature was defined and a predictive model with high diagnostic accuracy was constructed. Functional validation in vitro confirmed key molecular alterations in PD-MΦ, reinforcing their relevance to disease progression. Future work should focus on validating these findings in larger patient cohorts and employing spatial transcriptomics and in vivo functional assays to further characterise the role of PD-MΦ in tissue remodelling and immune regulation. Targeting the unique pathways and signalling networks of PD-MΦ may offer novel strategies for therapeutic intervention, paving the way for precision diagnostics and macrophage-targeted treatments in the clinical management of PD.

Conflict of interest

None disclosed.

Author contributions

Shaoyong Chen: Conceptualisation, Data curation, Investigation, Methodology, Software, Visualisation, Writing – original draft, Writing – review and editing. Jun Zhao: Data curation, Investigation, Resources, Validation, Writing – original draft. Jiayi Hang: Formal analysis, Investigation, Methodology, Software, Validation. Jianjia Tang: Formal analysis, Methodology, Software. Rong Xiang: Formal analysis, Methodology, Software. Siqin Zhang: Conceptualisation, Supervision, Project administration, Funding acquisition, Writing – review and editing. All authors reviewed and approved the final manuscript.

Ethics statement

This study employed commercially available cell lines (THP-1, ATCC® TIB-202™) and publicly available genomic datasets, and their use did not entail any harm to human or animal subjects. This study was thus exempt from formal ethics review by the Institutional Review Board of Guangxi Medical University. All procedures were conducted in accordance with ethical guidelines and institutional policies.

Funding

This work was supported by the Natural Science Foundation for Young Scholars of Guangxi Zhuang (2024GXNSFBA010143), the First-class discipline innovation-driven talent program of Guangxi Medical University, Young Elite Scientists Sponsorship Program by GXAST, and the 'Qingmiao' Talent Program of Guangxi.

Supplementary materials

Supplementary material associated with this article can be found in the online version at doi:10.1016/j.identj.2025.103983.

REFERENCES

1. Slots J. Periodontitis: facts, fallacies and the future. Periodontology 2000 2017;75(1):7–23.
2. Hajipour MJ, Saei AA, Walker ED, et al. Nanotechnology for targeted detection and removal of bacteria: opportunities and challenges. Adv Sci (Weinh) 2021;8(21):e2100556.
3. Kwon T, Lamster IB, Levin L. Current concepts in the management of periodontitis. Int Dent J 2021;71(6):462–76.
4. Janakiram C, Dye BA. A public health approach for prevention of periodontal disease. Periodontology 2000 2020;84(1):202–14.
5. Cui Y, Hong S, Xia Y, et al. Melatonin engineering M2 macrophage-derived exosomes mediate endoplasmic reticulum stress and immune reprogramming for periodontitis therapy. Adv Sci (Weinh) 2023;10(27):e2302029.
6. Sun X, Gao J, Meng X, Lu X, Zhang L, Chen R. Polarized macrophages in periodontitis: characteristics, function, and molecular signaling. Front Immunol 2021;12:763334.
7. Sima C, Viniegra A, Glogauer M. Macrophage immunomodulation in chronic osteolytic diseases-the case of periodontitis. J Leukoc Biol 2019;105(3):473–87.
8. Guo X, Huang Z, Ge Q, et al. Glipizide alleviates periodontitis pathogenicity via inhibition of angiogenesis, osteoclastogenesis and M1/M2 macrophage ratio in periodontal tissue. Inflammation 2023;46(5):1917–31.
9. Trzebanski S, Kim JS, Larossi N, et al. Classical monocyte ontogeny dictates their functions and fates as tissue macrophages. Immunity 2024;57(6):1225–1242.e6.
10. Shi J, Wu Z, Li Z, Ji J. Roles of macrophage subtypes in bowel anastomotic healing and anastomotic leakage. J Immunol Res 2018;2018:6827237.
11. Almubarak A, Tanagala KKK, Papapanou PN, Lalla E, Momen-Heravi F. Disruption of monocyte and macrophage homeostasis in periodontitis. Front Immunol 2020;11:330.
12. Das A, Sinha M, Datta S, et al. Monocyte and macrophage plasticity in tissue repair and regeneration. Am J Pathol 2015;185(10):2596–606.
13. Liu C, Zhang M, Yan X, et al. Single-cell dissection of cellular and molecular features underlying human cervical squamous cell carcinoma initiation and progression. Sci Adv 2023;9(4):eadd8977.
14. Chen Y, Wang H, Yang Q, et al. Single-cell RNA landscape of the osteoimmunology microenvironment in periodontitis. Theranostics 2022;12(3):1074–96.
15. Hanley CJ, Waise S, Ellis MJ, et al. Single-cell analysis reveals prognostic fibroblast subpopulations linked to molecular and immunological subtypes of lung cancer. Nat Commun 2023;14(1):387.
16. Korsunsky I, Millard N, Fan J, et al. Fast, sensitive and accurate integration of single-cell data with Harmony. Nat Methods 2019;16(12):1289–96.
17. Jin S, Guerrero-Juarez CF, Zhang L, et al. Inference and analysis of cell-cell communication using CellChat. Nat Commun 2021;12(1):1088.

18. Morabito S, Reese F, Rahimzadeh N, Miyoshi E, Swarup V. hdWGCNA identifies co-expression networks in high-dimensional transcriptomics data. Cell Rep Methods 2023;3(6):100498.
19. Hajishengallis G, Korostoff JM. Revisiting the Page & Schroeder model: the good, the bad and the unknowns in the periodontal host response 40 years later. Periodontology 2000 2017;75(1):116–51.
20. Seidel A, Seidel CL, Weider M, Junker R, Gölz L, Schmetzer H. Influence of natural killer cells and natural killer T cells on periodontal disease: a systematic review of the current literature. Int J Mol Sci 2020;21(24):9766.
21. Martínez-García M, Hernández-Lemus E. Periodontal inflammation and systemic diseases: an overview. Front Physiol 2021;12:709438.
22. Zhang M, Liu Y, Afzali H, Graves DT. An update on periodontal inflammation and bone loss. Front Immunol 2024;15:1385436.
23. Ali M, Huarte OU, Heurtaux T, et al. Single-cell transcriptional profiling and gene regulatory network modeling in Tg2576 mice reveal gender-dependent molecular features preceding Alzheimer-like pathologies. Mol Neurobiol 2024;61(2):541–66.
24. Cavalcante GC, Brito LM, Schaan AP, Ribeiro-Dos-Santos Â, de Araújo GS, On Behalf Of Alzheimer's Disease Neuroimaging I. Mitochondrial genetics reinforces multiple layers of interaction in Alzheimer's disease. Biomedicines 2022;10(4):880.
25. Zhao Q, Pang G, Yang L, Chen S, Xu R, Shao W. Long noncoding RNAs regulate the inflammatory responses of macrophages. Cells 2021;11(1):5.
26. Ahmad I, Naqvi RA, Valverde A, Naqvi AR. LncRNA MALAT1/microRNA-30b axis regulates macrophage polarization and function. Front Immunol 2023;14:1214810.
27. Boettner B, Van Aelst L. Control of cell adhesion dynamics by Rap1 signaling. Curr Opin Cell Biol 2009;21(5):684–93.
28. Bharuka T, Reche A. Advancements in periodontal regeneration: a comprehensive review of stem cell therapy. Cureus 2024;16(2):e54115.
29. Kotlyarov S, Kotlyarova A. Anti-inflammatory function of fatty acids and involvement of their metabolites in the resolution of inflammation in chronic obstructive pulmonary disease. Int J Mol Sci 2021;22(23):12803.
30. An Y, Tan S, Yang J, Gao T, Dong Y. The potential role of Hippo pathway regulates cellular metabolism via signaling crosstalk in disease-induced macrophage polarization. Front Immunol 2023;14:1344697.
31. Fang Y, Li X. Protein lysine four-carbon acylations in health and disease. J Cell Physiol 2024;239(3):e30981.
32. Liang H, Song K. Elucidating ascorbate and aldarate metabolism pathway characteristics via integration of untargeted metabolomics and transcriptomics of the kidney of high-fat diet-fed obese mice. PLoS One 2024;19(4):e0300705.
33. Samaniego R, Palacios BS, Domiguez-Soto Á, et al. Macrophage uptake and accumulation of folates are polarization-dependent in vitro and in vivo and are regulated by activin A. J Leukoc Biol 2014;95(5):797–808.
34. Zhang Y, Guo R, Kim SH, et al. SARS-CoV-2 hijacks folate and one-carbon metabolism for viral replication. Nat Commun 2021;12(1):1676.
35. Vicencio E, Nuñez-Belmar J, Cardenas JP, et al. Transcriptional signatures and network-based approaches identified master regulators transcription factors involved in experimental periodontitis pathogenesis. Int J Mol Sci 2023;24(19):14835.
36. Jurdziński KT, Potempa J, Grabiec AM. Epigenetic regulation of inflammation in periodontitis: cellular mechanisms and therapeutic potential. Clin Epigenet 2020;12(1):186.
37. Qian SJ, Huang QR, Chen RY, et al. Single-cell RNA sequencing identifies new inflammation-promoting cell subsets in Asian patients with chronic periodontitis. Front Immunol 2021;12:711337.
38. Xu Y, Wang L, Buttice G, Sengupta PK, Smith BD. Interferon gamma repression of collagen (COL1A2) transcription is mediated by the RFX5 complex. J Biol Chem 2003;278(49):49134–44.
39. Deng M, Odhiambo WO, Qin M, et al. Analysis of intracellular communication reveals consistent gene changes associated with early-stage acne skin. Cell Commun Signal 2024;22(1):400.
40. Faria MR, Hoshida MS, Ferro EA, Ietta F, Paulesu L, Bevilacqua E. Spatiotemporal patterns of macrophage migration inhibitory factor (Mif) expression in the mouse placenta. Reprod Biol Endocrinol 2010;8:95.
41. Subbannayya T, Leal-Rojas P, Barbhuiya MA, et al. Macrophage migration inhibitory factor—a therapeutic target in gallbladder cancer. BMC Cancer 2015;15:843.
42. Sun J, Nemoto E, Hong G, Sasaki K. Modulation of stromal cell-derived factor 1 alpha (SDF-1α) and its receptor CXCR4 in Porphyromonas gingivalis-induced periodontal inflammation. BMC Oral Health 2016;17(1):26.
43. Nagashima H, Shinoda M, Honda K, et al. CXCR4 signaling in macrophages contributes to periodontal mechanical hypersensitivity in Porphyromonas gingivalis-induced periodontitis in mice. Mol Pain 2017;13:1744806916689269.
44. Jiang YT, Xu LN, Zhao XR, et al. Explorations about the correlation between biological changes of meninges in periodontitis mice and cognitive impairment via single-cell RNA sequencing. Zhonghua Kouqiang Yixue Zazhi (Chinese Journal of Stomatology) 2024;59(6):595–603 (in Chinese).